Visible light Assisted Photocatalytic Degradation of DIPA Using Fe-Zn/TiO_2 Photocatalyst

by

Debra Adelina Chia Siew Fen

15261

Dissertation submitted in partial fulfillment of
the requirements for the
Bachelor of Engineering (Hons)
(Chemical)

SEPTEMBER 2014

Universiti Teknologi PETRONAS
Bandar Seri Iskandar
31750 Tronoh
Perak Darul Ridzuan.

CERTIFICATION OF APPROVAL

Visible light Assisted Photocatalytic Degradation of DIPA Using Fe-Zn/TiO_2 Photocatalyst

by

Debra Adelina Chia Siew Fen

15261

A project dissertation submitted
to the Chemical Engineering Programme
Universiti Teknologi Petronas
in partial fulfillment of
the requirements for the
BACHELOR OF ENGINEERING (Hons)
(CHEMICAL)

Approved by,

_____

(Assoc. Prof. Dr. Azmi B. Bustam @ Khalil)

UNIVERSITI TEKNOLOGI PETRONAS

TRONOH, PERAK

SEPTEMBER 2014

CERTIFICATION OF ORIGINALITY

This is to certify that I am responsible for the work submitted in this project, that the original work is my own except as specified in the references and acknowledgements, and that the original work contained herein have not been undertaken or done by unspecified sources of persons.

_____

(DEBRA ADELINA CHIA SIEW FEN)

Abstract

Diisopropanolamine (DIPA) is washed out into water as a result of the process of carbon absorption, contributing to a high chemical oxygen demand (COD). Water with high COD content is not suitable to be treated by biological method and hence, Advanced Oxidation Processes (AOPs) are gaining more and more interests. The efficiency of photocatalytic degradation of DIPA with the presence of visible light is tested with Fe-Zn/TiO_2. There are currently no studies found using this particular combination of dopant metals. There are two parts to this study; synthesis optimization and parametric optimization. Fe-Zn/TiO_2 photocatalysts were prepared using both co-precipitation (CP) and wet impregnation (WI) methods and also using different titania to determine the ones which give the highest photocatalytic activity. Parameters tested for the optimization includes metal composition (0-0.5), photocatalyst calcination temperature (200˚C, 300˚C, 400˚C), photocatalyst loading (0.05mg/mL, 0.1mg/mL, 0.5mg/mL), initial DIPA concentration (100ppm, 300ppm, 500ppm) and irradiation duration (1h). Fe-Zn/TiO_2 photocatalyst prepared by WI using anatase titania, with metal composition of 0.1Fe-0.4Zn and calcined at 300˚C was found to give the highest percentage of COD removal (66.5%). It was also concluded that the photocatalytic activity decreases with increasing initial DIPA concentration and increases with respect to time. The photocatalysts were characterized using TGA, SEM, FESEM, FTIR, XRD and BET.

TABLE OF CONTENT

LIST OF FIGURES

LIST OF TABLES

1.0 Introduction

1.1 Background

In gas streams from natural gas, exhaust gases and refinery gases, acid gases are present. One of the major acid gases of concern is carbon dioxide (CO_2). (Pellegrini, Moioli, & Gamba, 2011) CO_2 is considered to be the main contributor to the greenhouse effect, responsible for 60% of the increase in atmospheric temperature, commonly referred to as global warming. (Sayari, Belmabkhout, & Serna-Guerrero, 2011) Industrially, CO_2 is being removed from the gases through a process known as amine gas treating. This process involves using aqueous solutions of alkanoamines such as monoethanolamine (MEA), diethanolamine (DEA), methyldiethanolamine (MDEA) and diisopropanalamine (DIPA) to remove CO_2. (Omar, Ramli, & Khamaruddin, 2010)

The usage of aqueous solution of alkanoamines provides several advantages. The presence of amines dramatically influences the solubility of acid gases in water and significantly affects the rate of absorption of acid gases in aqueous solutions. (Pellegrini et al., 2011) Moreover, mass transfer is promoted by chemical reaction through the following steps i.e. diffusion of component from bulk gas phase to gas-liquid transfer, diffusion of reagents from gas-liquid interface to the bulk liquid phase, simultaneous reaction between dissolved gas and liquid reactant and lastly diffusion of reaction products in the bulk liquid phase promoted by the concentration gradient. (Moioli, Pellegrini, & Gamba, 2012) After the process of CO_2 capture, alkanoamines are being discharged into wastewater, causing a high content of COD. (Putri, Bustam, & Omar, 2011)

Residual alkanoamines from these processes may be carried out into wastewater and they may pose important implications with respect to the potential for production of toxic nitrosamines and nitramines through reactions between precursor amines and oxidants such as nitrite (NO_2^-). The risk of contamination of drinking water supplies by nitrosamines and nitramines are the foremost environment concern as 90% of nitrosamines and some of nitramines are believed to be carcinogenic. As for

environmental concerns, amines show slight to moderate toxicity to phytoplankton and bacteria. (Poste, Grung, & Wright, 2014)

In the recent two decades, Advanced Oxidation Processes (AOPs) for the treatment of wastewater have gained more and more interests due to its capability in degrading a wide range of organic and recalcitrant compounds. Studies have shown that Fenton oxidation and photocatalysis are capable of degrading these alkanoamines.

There is one major advantage of photocatalysis over Fenton oxidation which is the recyclability of the catalysts. In a study conducted to enhance the photocatalytic performance, the recyclability and ease of collection of photocatalysts have been put to test. The process was repeated for 10 cycles and it was shown that the degradation capability reduces from 98.83% to 96.32%. Evidently, the degradation efficiency did not change much, revealing excellent recyclability stability. (Li et al., 2014)

Photocatalysis is a heterogenous process based on the double aptitude of the photocatalyst to simultaneously adsorb reactants and absorb photons. The presence of UV or visible light excites electrons from the valence band to the conduction band, generating an electron pair (e^-, h^+). This electron pair leads to the formation of hydroxyl radicals ($OH^\bullet$) which will react to degrade the alkanoamines. (Alfons & Kim, 2003; Ohtani, 2010)

1.2 Problem Statement

Due to the increasing usage of amine-based CO_2 capture technology, there is a need to develop cheap and efficient methods to degrade the residual amines. One of the alkanoamines used, DIPA, poses great concern due to its toxicity, which contributes to a high COD content in wastewater. Shell, one of Malaysia's largest oil and gas companies, utilizes DIPA in two of its technologies namely ADIP-D and SULFINOL-D with the purpose of removing CO_2 and H_2S. AOPs such as Fenton oxidation and photocatalysis have proven to be efficient in degrading DIPA. (Putri et al., 2011; Ramli, Chong, & Omar, 2014; N Riaz et al.; Zhi, Bustam, Riaz, & Shariff, 2014)The cost effectiveness of photocatalysis is showing great interests due to the recyclability of the photocatalysts. Using TiO_2 semiconductor as a photocatalyst has been reported very efficient to degrade a range of pollutants. However, there is a limitation to its usage due to its large band gap energy which is photoactive only in the light wavelength of 388nm or less (Yoong, Chong, & Dutta, 2009). The activity can be increased by doping TiO_2 with metal ions, non-metal ions and co-doping. DIPA has been successfully degraded using bimetallic photocatalysts i.e. Cu-Fe and Cu-Ni (Ramli et al., 2014; N Riaz et al.) Based on literature, there have been no previous studies made using Fe-Zn/TiO_2 photocatalyst. The interest of this study is to investigate the effectiveness of Fe-Zn/TiO_2 photocatalysts in the degradation of DIPA.

1.3 Objectives and Scope of Study

1.3.1 Objectives

- To optimize the synthesis of Fe-Zn/ TiO_2 photocatalysts
- To study the photocatalytic degradation of DIPA in the presence of Fe-Zn/TiO_2 under visible light source

1.3.2 Scope of study

1.3.2.1 Parameters for Photocatalyst Synthesis Optimisation

- Method of Preparation
- Type of Titania Used

1.3.2.2 Parameters for Photocatalysts Preparation

- Fe:Zn/TiO_2 metal composition (0-0.5)
- Calcination temperature (200˚C, 300˚C, 400˚C)

1.3.2.3 Parameters for Photocatalytic Activity

- Initial DIPA concentration (100, 300, 500 ppm)
- Irradiation time (1hour)

2.0 Literature Review

In order to produce safe drinking water, treatments are done to degrade these alkanoamines. Conventional methods include biological treatments such as aerobic and anaerobic biodegradation. (Deshai Botheju et al.) However, these biological wastewater treatments can only degrade COD level of below 1000mg/L. Wastewater containing DIPA is discovered to have high COD, where in a natural gas plant, it can go up to about 5000 and a maximum of 25000 mg/L. Thus, chemical treatments especially AOPs are preferred due to high efficiency as well as cost effectiveness. (Putri et al., 2011). As of the advantage of recyclability of catalysts, photocatalytic oxidation is chosen to be the subject of our study.

2.1 Photocatalytic oxidation

Photocatalysis is a heterogeneous process in which a solid-state metal catalyst is illuminated with photons with higher energy or equal to its band gap to create photo-electrons (Liu, Zeng, Jiang, Zhang, & Li) photo-holes (h^+). (Herrmann, 2010) The positive holes oxidize pollutants directly or react with water to produce OH radicals. (Ahmed, Rasul, Martens, Brown, & Hashib, 2010)

2.1.1 TiO_2 Photocatalyst

TiO_2 is the preferred catalyst due to its stability under various conditions, excellent resistance to chemical and photochemical corrosion in aqueous environment, its reactivity towards both light and water, its high potential to produce radical, its easy available and low price. (Alfons & Kim, 2003; Yoong et al., 2009)

According to a review by Thiruvenkatachari et al, the photocatalytic activity for TiO_2 has been reported to be more efficient as compared to CdS catalyst for the degradation of phenol. There has also been a study reporting that under similar study conditions, TiO_2 showed better efficiency in comparison to α-Fe_2O_3, ZrO_2, CdS, WO_3 and SnO_2. However, there were contradicting reports on whether TiO_2 or ZnO is a better photocatalyst. (Thiruvenkatachari, Vigneswaran, & Moon, 2008)

However, pure TiO_2 is only photoreactive under visible light in which it can only absorb near-UV range of approximately 338 nm or less. Given that solar light consist of ~5% UV, ~43% and ~52% harvesting infrared, the utilization of natural solar light for the photocatalytic activity can be done if the band gap response of TiO_2 is tuned into the visible light region. (Kumar & Devi, 2011) The usage of natural solar light could have a significant impact in the cost aspect.

For this purpose, TiO_2 is modified by various strategies like coupling with a narrow band gap semiconductor, metal ion/non-metal ion doping, co-doping with two or more foreign ions, surface sensitization by organic dyes and metal complexes, surface fluorination, and noble metal deposition. (Kumar & Devi, 2011) Studies have been conducted by incorporating transition metal oxides such as Fe, Zn, Cu, Ni and V (Yoong et al., 2009), non-metal ions like nitrogen and fluorine- TiO_2 (NF- TiO_2), phosphorus and fluorine-TiO_2 (PF- TiO_2) and sulfur-TiO_2 (S- TiO_2) (Zhao et al., 2014), semiconductors $SrTiO_3$ (Wang et al., 2014) and co-doping like Cu-Fe/ TiO_2 (Ramli et al., 2014) and Cu-Ni/ TiO_2 (N Riaz et al.) to prove their efficiencies. Doping lessens the band gap of TiO_2 for the photo-excitation and at the same time, reduces the recombination rate of the electron-hole pairs. (Yoong et al., 2009)

2.1.2 Fe/TiO_2 Photocatalyst

Doping TiO_2 with metal ions has proven to be efficient for improving visible light photoactivity with hindered recombination of the electron-hole pairs. Fe^{3+} dopant has a unique half-filled electronic structure. When Fe^{3+} traps electron and holes, it changes to Fe^{2+} and Fe^{4+} respectively. Fe^{2+} and Fe^{4+} however are not as stable as Fe^{3+} and therefore tend to detrap the electron and holes to adsorbed oxygen and surface hydroxyl group, suppressing the regeneration of electron pairs. (Kumar & Devi, 2011)

In a study reported by Murakami et al., different metal ions; Fe^{3+}, Cu^{2+}, Ni^{2+} and Cr^{3+} were used to doped TiO_2 which were then used as photocatalysts in the oxidation of acetaldehyde. Fe^{3+} showed the highest catalytic activity, followed by Cu^{2+}, Ni^{2+} and Cr^{3+}. It was concluded that Fe^{3+} served as a higher electron acceptor due to its higher positive reduction potential. (Kumar & Devi, 2011)

Iron-doped titanium dioxide (Fe/TiO_2) has been used to degrade various contaminants effectively such as methyl ter-butylether (MTBE) (Safari, Nikazar, & Dadvar, 2013), phenol (Tryba, Morawski, Inagaki, & Toyoda, 2006), ammonia (Obata et al., 2014), formic acid (Arana et al., 2001), organic dyes (Qi, Wang, Zhuang, Yu, & Li, 2005) etc.

2.1.3 Zn/TiO_2 Photocatalyst

It has been reported that ZnO is as reactive as, if not more reactive than TiO_2 with similar band gap energy of 3.2eV. According to Sobana and Swaminathan, ZnO showed higher efficiency than TiO_2 in the degradation of Acid Red 18 under UV radiation, due to its larger surface area; ZnO ($10m^2/g$) over anatase TiO_2 ($8.9m^2/g$). Another study by Talebian and Nilforoushan reported higher efiiciency of ZnO over TiO_2 in the degradation of methylene blue under UV radiation. (Ahmed et al., 2010)

Zn doped titania has been used for the degradation of mainly, dyes such as methyl orange (Chen et al., 2008; Siuleiman et al.) and Rhodamine B dye (Pei & Leung, 2013).

2.1.4 Fe-Zn/TiO_2

Co-doping has shown to have significant effects in increasing the photocatalytic activities as compared to single ion-doped or pure TiO_2. Interactions between the dopants change the elctron-holes recombination dynamics and thus, shift the band gap toward the visible light region. The enhanced visible light absorbance increases the solubility limits of dopants. (Kumar & Devi, 2011)

Fe-Zn/TiO_2 has been used in a study for the degradation of phenol. It was proven that the co-doped TiO_2 is more effective than TiO_2 alone. The optimum pH was found to be in the range of 5-9. (Yuan, Jia, & Zhang, 2002)

There were not a lot of studies found using this combination of metals as dopants.

2.1.4 Photocatalystic oxidation on DIPA

Bimettalic Cu-Ni/ TiO_2 was used as the photocatalyst and showed higher efficiency in the degradation of DIPA as compared to bare TiO_2. Results showed highest COD removal of 86.82% was obtained using photocatalyst calcined at 200˚C. It was reported

that photocatalytic activity was higher at alkanine conditions, increased with photocatalyst loading and decreased with increasing initial DIPA concentration. (N Riaz et al.)

Another study used bimettalic Cu-Fe/ TiO_2 in the degradation of DIPA. It also showed higher efficiency than bare TiO_2 in comparison with band gap; Cu-Fe/TiO_2 (2.77eV) and TiO_2 (3.05eV). It was reported that the highest DIPA degradation was at 92% at an optimum pH of 8. (Ramli et al., 2014)

There have been no reported studies in the literature on the degradation of DIPA using Zn-Fe/TiO_2.

3.0 Methodology/ Project Work

3.1 Materials

Diisopropanolamine (1,1-Iminodi-2-propanol, Merck) was used as model pollutant for photocatalytic degradation study.

For photocatalyst preparation, Iron (III) nitrate nonahydrate, $Fe(NO_3)_2 \cdot 9H_2O$ (Merck 10388) and $Zn(NO_3)_2.6H_2O$ shall be used as dopant metal salts. Titanium (IV) oxide, mixture of rutile and anatase and titania (Sigma-Aldrich), anatase (Aldrich) shall be used as the support which also act as the semiconductor in photocatalysis. Sodium hydroxide, NaOH (Merck, 95% purity) shall be used as precipitating agent. All chemicals shall be used as received.

IUPAC name	Diisopropanolamine
Other names	1,1'-iminobis-2-propano; 1,1'-iminodi-2-propano; 1,1'-Imino-2-propanol; 2,2'-Dihydroxy-dipropyl-amine; 2-Propanol, 1,1'-iminobis-; 2-Propanol, 1,1'-iminodi-; Bis(2-propanol)amine; Di(2-hydroxy-n-propyl) amine
CAS number	110-97-4
Molecular formula	C6H15NO2
Molar mass	133.19 g/mol
Appearance	Colorless liquid or white to yellow crystalline solid with an odor of dead fish or ammonia
Solubility in water	Soluble
Chemical structure	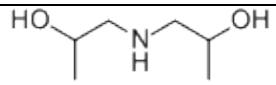

Table 1 Specification of Model Amine: DIPA

3.2 Experimental Start-up

Stock solutions of different reagents required to conduct experiments were prepared. 1000ppm of DIPA solution is initially prepared and further diluted to desired concentrations with distilled water; whereas initial concentration of H_2O_2 reagent is prepared at 1.0M.

Experiments were conducted in batch mode in a batch reactor with provisions of sampling, temperature and pH probes and with the presence of 300W light.

3.3 Experiment Procedure for Photocatalytic Experiment

3.3.1 Experiment Start-up

3.3.1.1 Preparation of Photocatalysts

By Co-precipitation

A series Fe-Zn/TiO_2 photocatalysts with different metal composition (0-0.5) were prepared using TiO_2 as support via coprecipitation (CP) method (Nadia Riaz, Chong, Man, Khan, & Dutta, 2013). Appropriate amount of metal salts was dissolved in distilled water, followed by the addition of TiO_2 with continuous stirring for 1 hour prior to precipitation with 0.25 M NaOH. The preparation temperature was maintained in the range from 8 to 10 °C. The final pH was kept at 12, and the mixture was aged for 1 day. The precipitates were filtered and dried in an oven at 75 °C overnight. The raw photocatalysts were ground into a fine powder, kept in an airtight glass bottle, and stored in a desiccator.

By Wet Impregnation

A series Fe-Zn/TiO_2 photocatalysts with different metal composition (0-0.5) were prepared using TiO_2 as support via wet impregnation (WI) method. Weighted amount of titania are added in respective amount of metal salt solution. After continuous stirring of 1 hour, the mixture is stirred in a water bath of 80˚C. Temperature is monitored throughout until the mixture turns slurry. It is then placed overnight in the oven at 120 ˚C. The raw photocatalysts were ground into a fine powder, kept in an airtight glass bottle, and stored in a desiccator.

The photocatalysts were further calcined at different temperature (300-500°C). The best performing photocatalysts were identified from the screening process (higher % COD removal) were selected for further investigation.

3.3.1.2 Flowchart representation for preparation of photocatalysts

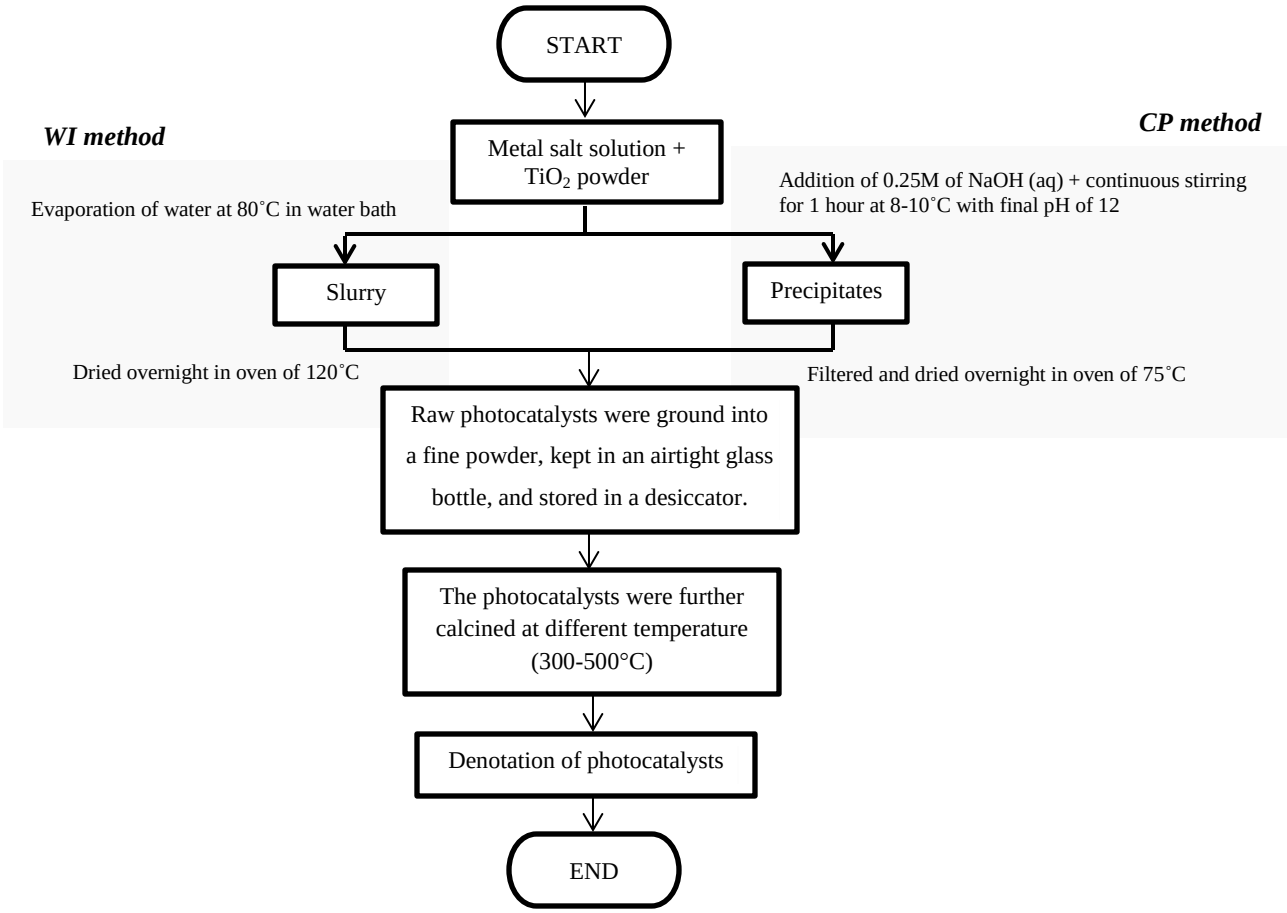

Figure 1 Flowchart representation for preparation of photocatalysts

3.3.2 Measurements of photocatalytic activities

Photocatalytic activity of the prepared photocatalysts was evaluated by monitoring the photocatalytic degradation of DIPA in aqueous solution under visible light irradiation. For a typical experiment, photocatalysts were weighed and mixed with distilled water and then ultrasonicated for 5 min using an ultrasonicator followed by the addition of alkanolamie solution (final concentration adjusted accordingly and photocatalyst loading of 1 g•L^{-1} and total volume of 100 ml). The suspension was stirred in the dark for 30 minutes and later this suspension was illuminated for 1 h using the 300W halogen lamp as the visible light source. Reaction study was carried out at atmospheric pressure and room temperature (at 25±1^{0}C) that was controlled by continuous cooling air. Samples were collected at different intervals and which were immediately centrifuged twice to remove suspended solid photocatalyst and monitored for further analysis. For the photodegradation experiments at different pH, the initial pH of the reaction suspension was adjusted by the addition of NaOH or HCl solutions. Schematic diagram of photocatalytic oxidation of DIPA is presented in Figure 2.

The degradation of alkanolamine was characterized by percent mineralization by measuring the chemical oxygen demand (COD) using Hach UV-Vis spectrophotometer (DR 3900) to measure the COD concentration (mg.L^{-1}) for the reaction samples. In order to determine the mineralization efficiency of photocatalyst, COD removal (%) was calculated as follows;

$$COD\ removal\ (\%) = \frac{COD_0 - COD_t}{COD_0} \times 100\% \qquad \text{(Equation 1)}$$

where COD_0 = initial COD in ppm and COD_t = final COD concentration in ppm at different time intervals during reaction.

3.3.3 Photocatalysts characterization

It is important to characterize the calcined photocatalysts in order to determine their chemical and physical properties and then to relate these properties to their photocatalytic performance. In this study, photocatalysts will be characterized using Thermogravimetric Analysis (TGA), FTIR (Perkin Elmer Spectrum one FTIR

spectrophotometer), XRD (Bruker D8 Advance Diffractometer), FESEM (Supra55VP), DR-UV–Vis (Shimadzu) and BET surface area analyzer (BELSORP, Japan).

Thermogravimetric Analysis (TGA) was carried out to study the thermal stability of the photocatalysts. Fourier transform Infra-red (FTIR) investigates the surface functional groups. A disc containing 1 % activated or inactivated carbon with 99% KBr shall be prepared and placed inside the analysis chamber and exposed to infra-red light wavelength ranging from 400 to 400 cm^{-1}. The phases present in the photocatalysts shall be investigated using XRD with Cu Kα radiation (40 kV, 40 mA) at 2θ angles from 10° to 80°, with a scan speed of 4° min^{-1}. Surface morphology such as crystallite particle shape, size, and particle size distribution of the produced photocatalyst shall be investigated using Field Emission electron microscopy (FESEM). The BET surface area, pore volume, and pore diameter of the photocatalysts shall be analyzed using BET surface area analyzer. The summary of the Photocatalysts characterization is presented in Table 2.

Analysis	**Model**	**Function**
Thermogravimetric Analysis (TGA)	Pyris 1	Thermal stability
Fourier-Transformed Infrared Spectroscopy (FTIR)	Perkin Elmer Spectrum one FTIR spectrophotometer	Species (functional group) identification
X-ray Diffraction (XRD)	Bruker D8 Advance Diffractometer	Crystal phases and Crystallite sizes
Field Emission electron microscopy (FESEM)	Supra55VP	Morphology
N_2-physisorption (BET)	BELSORP, Japan	Surface area, pore volume, and average pore diameter

Table 2 Characterization of Photocatalysts

3.4 Gantt Chart/ Project Milestone

3.4.1 FYP 1

No	Detail Work	1	2	3	4	5	6	7	8	9	10	11	12	13	14
1	Project title selection and meeting with FYP coordinator and supervisor														
2	Preliminary Research work and proposal preparation														
3	Extended proposal submission and proposal defence							★							
4	Confirmation of available resources														
5	Preparation of calibration curve														
6	Preparation of photocatalysts using co-precipitation method														
7	Photocatalysts Calcination														
8	Start photocatalytic experiment														
9	Submission of Interim Draft Report												★		
10	Submission of final Interim Report													★	

Table 3 Gantt Chart (FYP1)

3.4.2 FYP 2

No	Detail Work	1	2	3	4	5	6	7	8	9	10	11	12	13	14
1	Preparation of photocatalysts using wet impregnation method (rutile & anatase)														
2	Calcination of photocatalysts														
3	Photocatalytic experiment														
4	Preparation of photocatalysts using wet impregnation method (anatase)														
5	Calcination of photocatalysts														
6	Photocatalytic experiment														
7	SEM														
8	Parametric optimization														
9	Submission of progress report								★						
10	TGA														
11	FTIR														
12	BET														
13	XRD														
14	FESEM														
15	Pre-Sedex										★				
16	Submission of draft (final report)											★			
17	Submission of dissertation (soft bound)												★		
18	Submission of technical paper												★		
18	Viva													★	
18	Submission of dissertation (hard bound)														★

Table 4 Gantt Chart (FYP 2)

4.0 Results and Discussion

4.1 Synthesis Optimisation

There are two parts to this optimization where photocatalysts were prepared using different methods; co-precipitation (CP) and wet impregnation (WI) and then screened through another parameter which is the type of titania used; mixture of rutile and anatase and anatase alone.

4.1.1 Effect of Method of Preparation

A set of 5wt% Fe-Zn/TiO_2 photocatalysts are prepared using CP method with different metal compositions. $Fe(NO_3)_2.9H_2O$ (Merck 10388) and $Zn(NO_3)_2.6H_2O$ were used as dopant salts whereas Titanium (IV) dioxide, mixture of rutile and anatase (Sigma-aldrich) was used as support to produce the photocatalysts. This set of photocatalysts was then calcined at 300˚C. Reaction studies were carried out using 300 ppm DIPA solution.

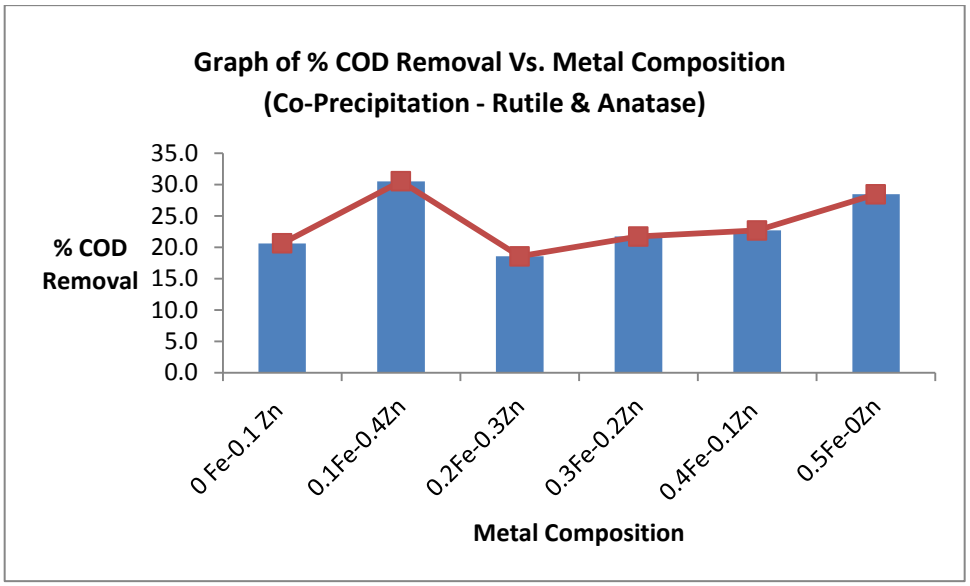

Figure 2 Graph of % COD Removal Vs. Metal Composition (Co-precipitation - Rutile & Anatase)

The following results were obtained showing that the photocatalyst containing metal composition of 0.1Fe-0.4Zn was the most effective with 30.5% COD removal.

Another set of 5wt% photocatalysts using the same materials and of the same range of metal compositions was next prepared using another method, which is the WI method. Reaction studies were carried out in similar condition.

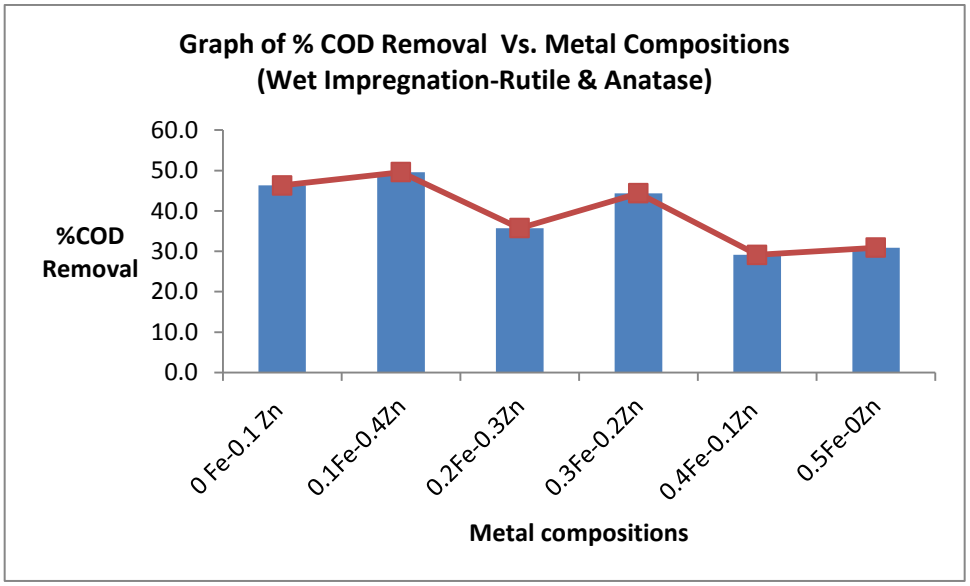

Figure 3 Graph of % COD Removal Vs. Metal Compositions (Wet Impregnation-Rutile & Anatase)

Results showed that similar metal composition which is 0.1Fe-0.4Zn had the highest % COD removal which was 49.6%.

By comparing the two graphs, it is concluded that all compositions of photocatalysts prepared using WI method showed higher COD removal percentage as compared to the ones prepared by using CP method.

4.1.2 Effect of Type of Titania Used

Considering WI to be the better method of producing the photocatalysts, another parameter which was the type of titania used, was put to test. Another set of 5wt% photocatalysts with the same range of metal composition was prepared. Nonetheless, instead of using titania of mixture of rutile and anatase, titania of anatase (Aldrich) was used. The set of photocatalysts were also calcined at 300˚C. Reaction studies were carried out under the same condition of 300ppm DIPA solution.

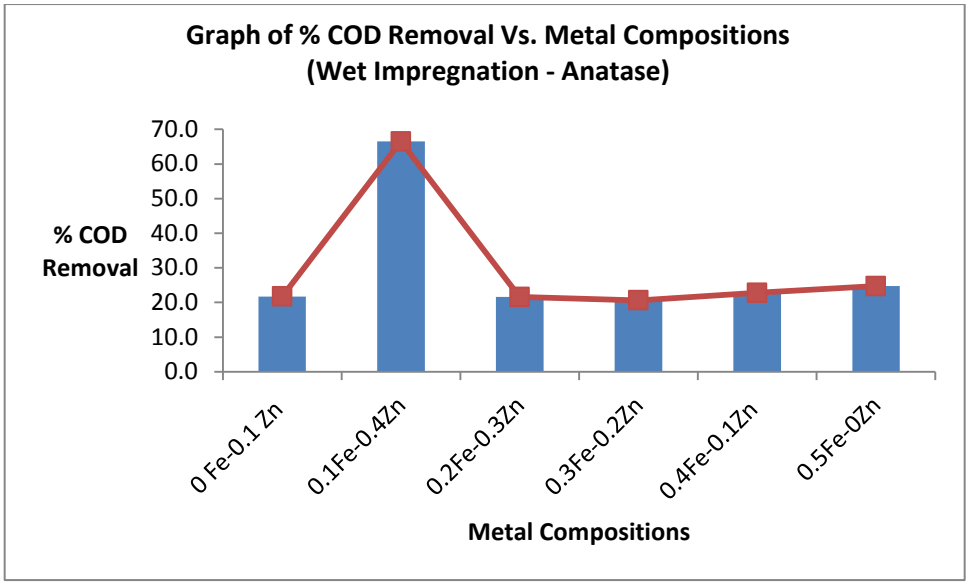

Figure 4 Graph of % COD Removal Vs. Metal Compositions (Wet Impregnation - Anatase)

Similarly, the photocatalyst of metal composition of 0.1Fe-0.4Zn exhibit the highest COD removal which is 66.5%. As compared to the previous was which was prepared titania, mixture of rutile and anatase, this one showed a higher COD removal percentage.

We hereby arrive at two conclusions:

1. Photocatalyst of Fe-Zn/TiO_2 showed the highest COD removal when prepared by wet impregnation method, using titania of anatase only
2. The best metal composition is 0.1Fe-0.4Zn.

4.2 Parametric Optimization

The best photocatalyst, 0.1Fe-0.4Zn/TiO_2 was used to run all the following reaction studies with different process parameters; irradiation duration (1h), photocatalyst calcination temperature, photocatalyst loading and initial DIPA concentration.

4.2.1 Effect of Photocatalyst Calcination Temperature

The photocatalyst of 0.1Fe-0.4Zn/TiO_2 was calcined at three different temperatures; 200˚C, 300 ˚C and 400 ˚C. They are then screened for photocatalytic degradation of DIPA at 300ppm under visible light irradiation.

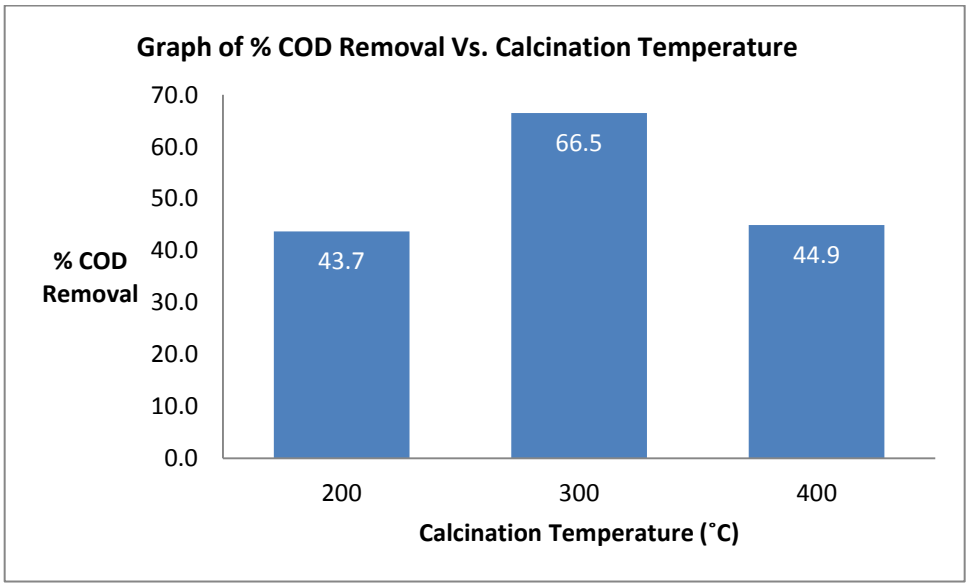

Figure 5 Graph of % COD Removal Vs. Photocatalyst Calcination Temperature

The % COD removal for different calcination temperatures are 45.3%, 66.5% and 46.5% respectively for 200˚C, 300˚C and 400˚C. Photocatalyst of 0.1Fe-0.4Zn/TiO_2 gives highest percentage of COD removal when calcined at 300˚C as compared to that at 200˚C and 400˚C. This shows that the photocatalytic activity decreases with increased calcination. It has been reported in previous study that higher calcination temperature may induce the growth of particles which reduce the contact area of particles for photocatalytic reactions. (Liu, Wang, Zheng,

Yang, & Sun, 2014) However, if the temperature gets too high, the photocatalytic activity decreases. This can be due to decomposition of the metals.

4.2.2 Effect of Initial DIPA concentration

To study the effect of initial DIPA concentration on the photocatalytic activity, the amount of photocatalyst loading is fixed at 1mg/mL. Initial COD percentages were taken at the beginning of the reaction and the final ones were again taken after an hour of irradiation under visible light. Plot of % COD removal against DIPA concentration is shown below.

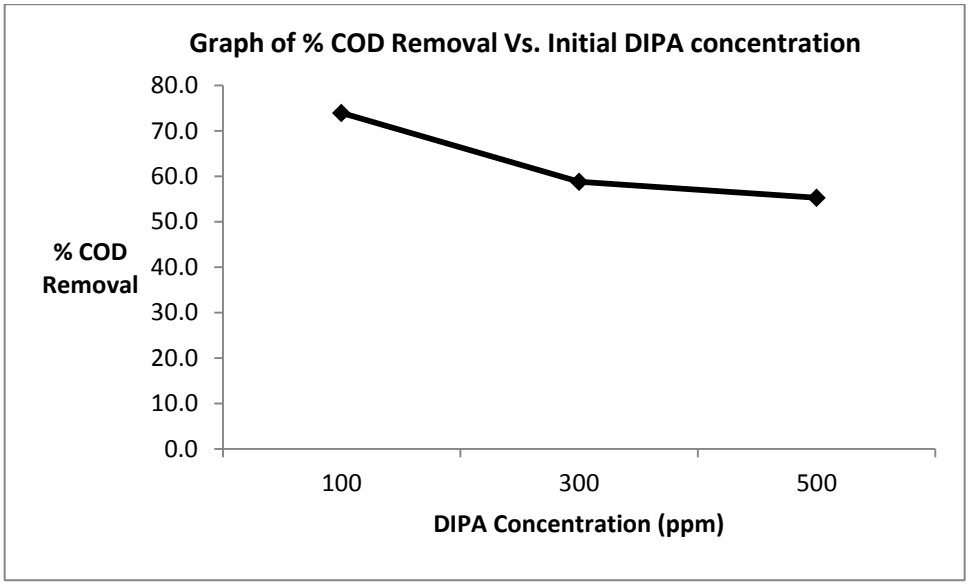

Figure 6 Graph of % COD Removal Vs. Initial DIPA Concentration

It is observed that the photocatalytic activity decreases with increasing DIPA concentration. Comparatively, the photocatalysts work better on lower DIPA concentration.

4.2.3 Effect of Irradiation Time

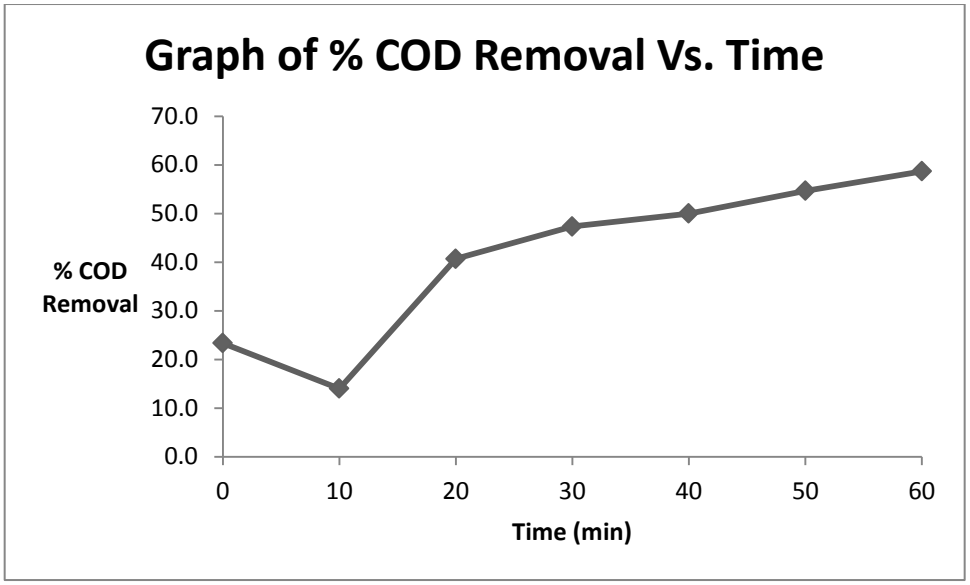

Figure 7 Graph of % COD Removal Vs. Time

Reaction was run at 300ppm DIPA solution with 0.1Fe-0.4Zn/TiO_2 photocatalyst calcined at 300˚C. The photocatalytic degradation of DIPA with time is shown in the figure above. Samples are taken every 10 minutes from T=0, when the light reaction is started till T=60. It is evident that the photocatalytic degradation increases with time.

4.3 Photocatalyst Characterisation

4.3.1 Photocatalyst morphology

SEM micrographs together with the EDS graphs of bare anatase TiO_2 and 0.1Fe-0.4Zn/TiO_2 (anatase) at different calcination temperature of 200˚C, 300˚C and 400˚C are displayed below.

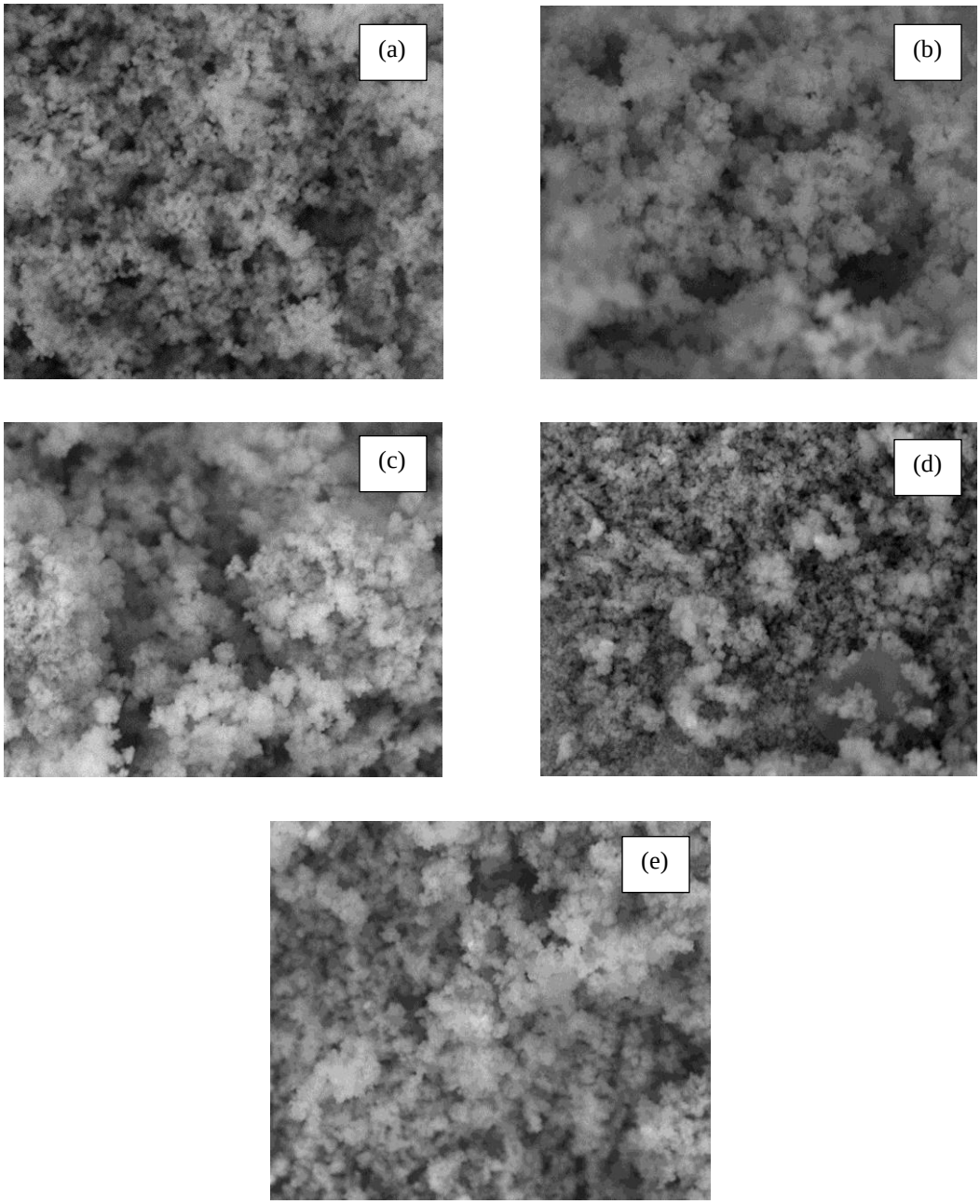

Figure 8 SEM micrographs of 15kx magnification of (a) bare anatase TiO2 (b)0.1Fe-0.4Zn/ TiO2 (c) 0.1Fe-0.4Zn/ TiO2 calcined at 200˚C (d) 0.1Fe-0.4Zn/ TiO2 calcined at 300˚C and (e) 0.1Fe-0.4Zn/ TiO2 calcined at 400˚C.

Figure above shows SEM micrographs of 15kx magnification of (a) bare anatase TiO_2 (b)0.1Fe-0.4Zn/ TiO_2 (c) 0.1Fe-0.4Zn/ TiO_2 calcined at 200˚C (d) 0.1Fe-0.4Zn/ TiO_2 calcined at 300˚C and (e) 0.1Fe-0.4Zn/ TiO_2 calcined at 400˚C.

All micrographs show irregular shaped crystalline which varies in sizes. As compared to the bare titania, the photocatalysts which are doped with metals show more agglomerations. It can be seen that the photocatalysts calcined at 200˚C and 400˚C contain more agglomerations of particles.

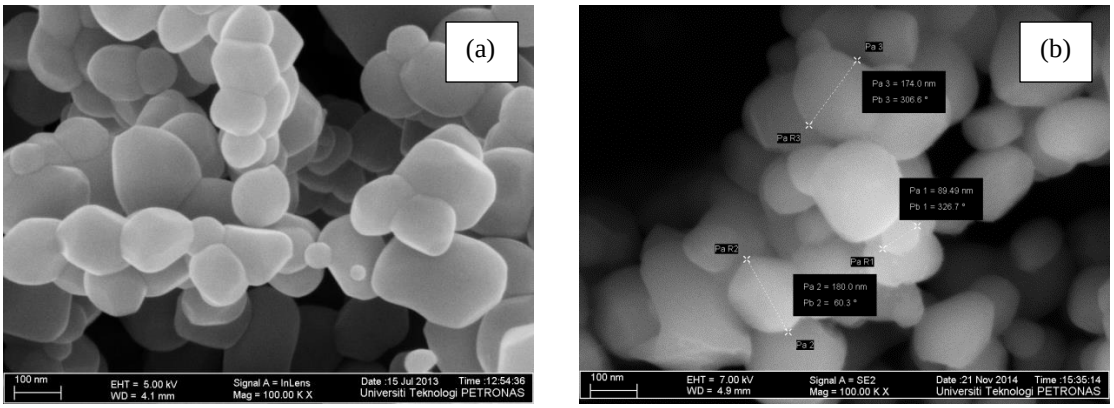

Figure 9 FESEM photographs of (a) bare TiO_2 and (b) 0.1Fe-0.4Zn/TiO_2 calcined at 300˚C

Field-Emission Scanning Electron Microscopy (FESEM) photographs of bare TiO_2 and the best performing photocatalyst, 0.1Fe-0.4Zn/TiO_2 are shown in the figure above. The photocatalyst shows more agglomerations as compared to bare titania, indicating the deposition of metals. Particles of the photocatalyst range between 89.49 to 180 nm.

4.3.2 X-Ray Diffraction (XRD)

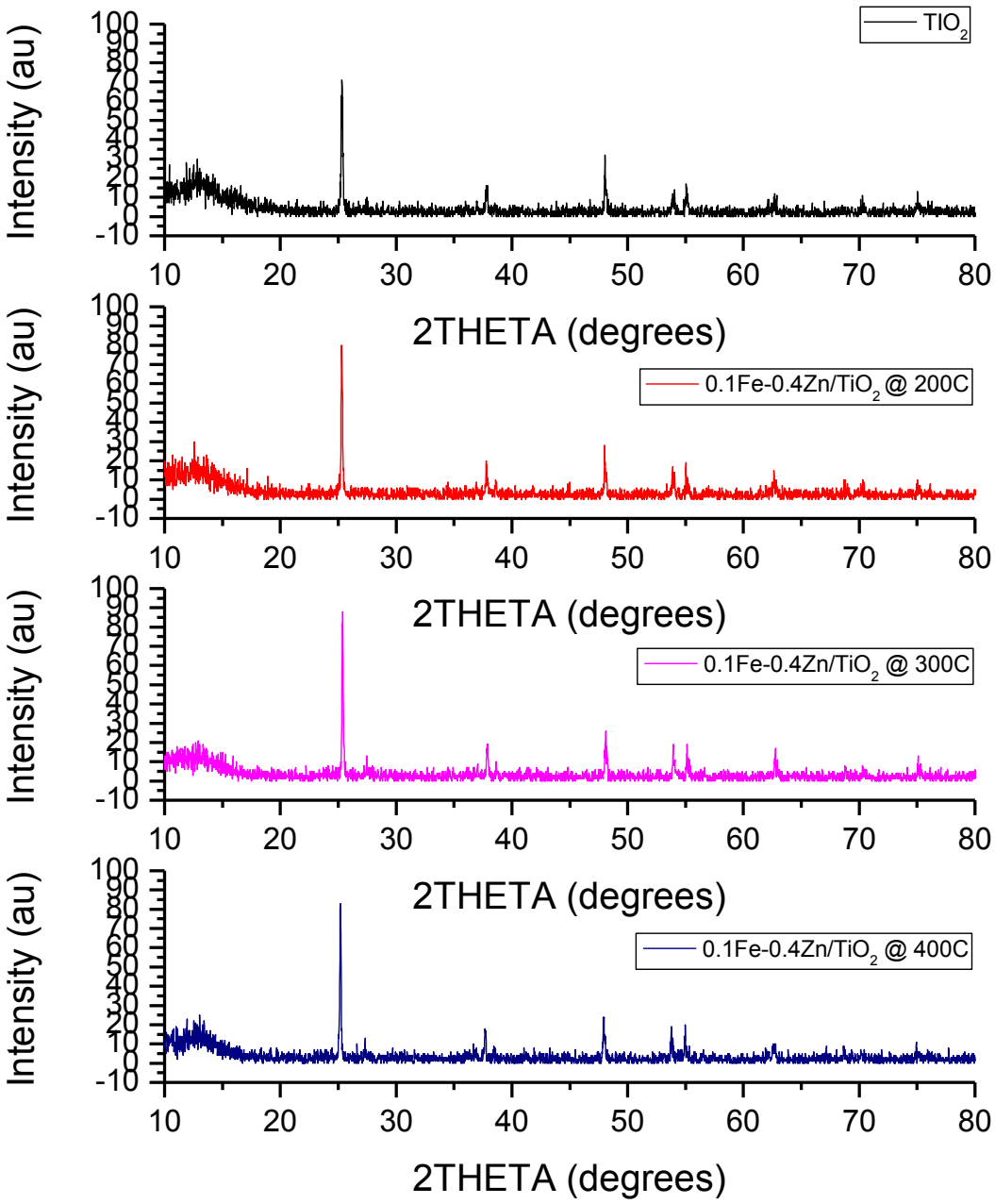

Figure 10 Graphs of intensity Vs. 2Θ for (a) bare TiO_2 (b) 0.1Fe-0.4Zn/TiO_2 Calcined at 200˚C (c) 0.1Fe-0.4Zn/TiO Calcined at 300˚C and (d) 0.1Fe-0.4Zn/TiO_2 Calcined at 400˚C

The XRD patterns for bare TiO_2 and 0.1Fe-0.4Zn/ TiO_2 of different calcination temperature; 200˚C, 300˚C and 400˚C are shown in the figure above. The XRD patterns for all are similar with the main peak at 2ϴ = 25.4 corresponding to anatase phase. No phase transition was observed for the calcined photocatalysts.

4.3.3 Thermogravimetric Analysis (TGA)

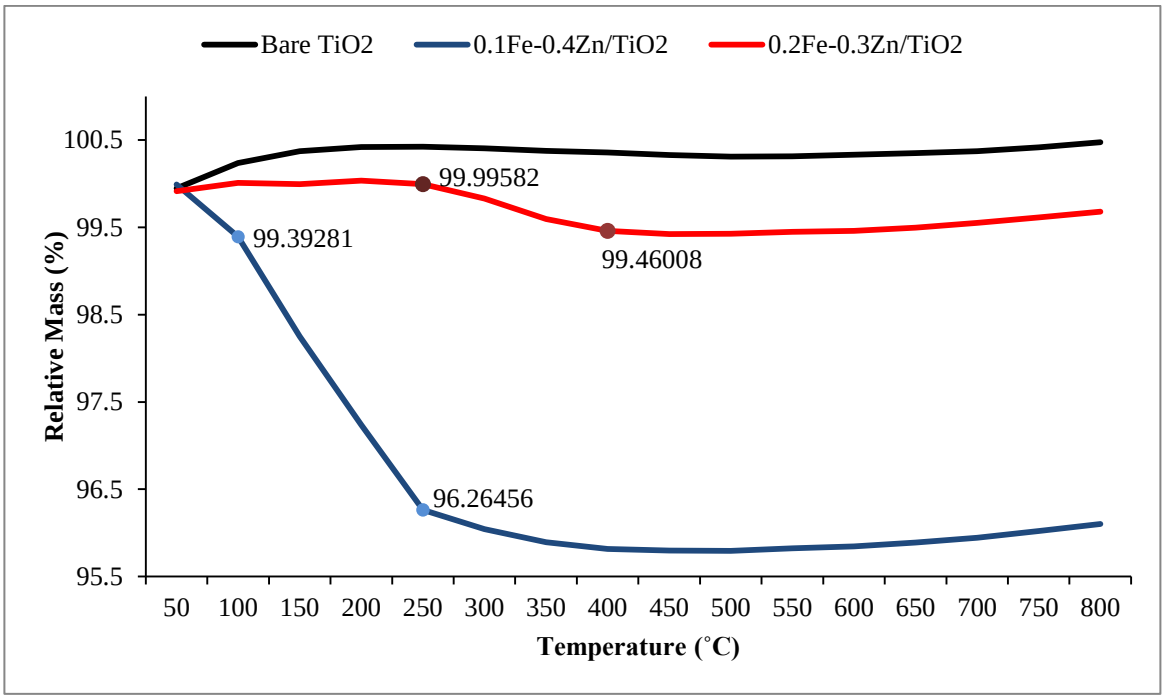

Figure 11 Graph of Relative Mass Vs. Temperature

A comparison of the weightloss profile of bare TiO2 and Fe-Zn doped Photocatalysts is shown in Figure. Fe-Zn/TiO_2 photocatalysts were selected based on their photodegradation performance. The above figure shows the thermogram of bare titania (Anatase), the best performing photocatalyst and the worst performing catalyst from the same series, prepared using wet impregnation with anatase titania; 0.1Fe-0.4Zn/TiO_2 and 0.2Fe-0.3Zn/ TiO_2.

From the curve of bare TIO_2, no steps were identified. As for the other two curves, two steps were identified for each. For the curve of 0.1Fe-0.4Zn/TiO_2, first step represents the water evaporation, identified between 50-100 while the second abrupt step from 100˚C and 250˚C represents the decomposition of metal precursor, with total weight loss

of 3.12825%. As for 0.2Fe-0.3Zn/TiO_2, similar trend was observed with less steeper steps compared to the previously discussed sample. The second slope was identified between 250˚C and 400˚C with a total weight loss of 0.57482%. Comparing the thermograms, the photocatalyst of 0.1Fe-0.4Zn/TiO_2 shows a steeper weight loss profile.

4.3.4 Fourier-Transformed Infrared Spectroscopy (FTIR)

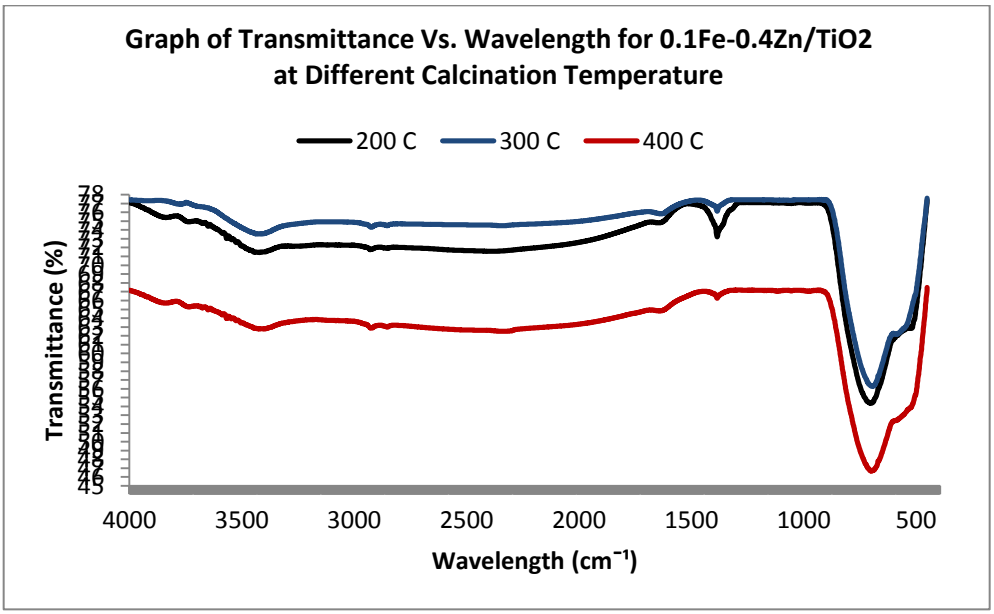

Figure 12 Graph of Transmittance Vs. Wavelength for 0.1Fe-0.4Zn/TiO2 at Different Calcination Temperature

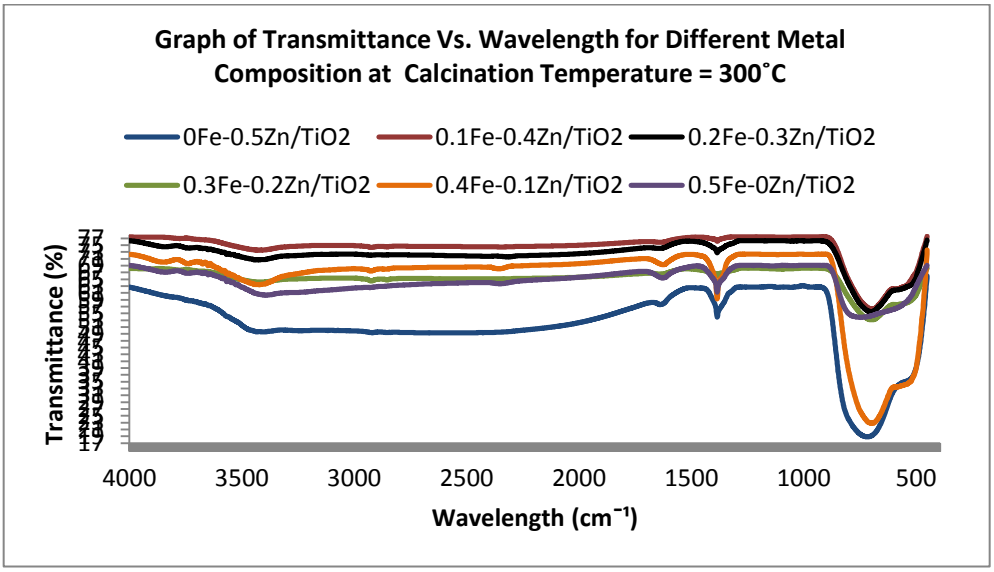

Figure 13 Graph of Transmittance Vs. Wavelength for Different Metal Composition at Temperature = 300˚C

Peaks (cm^{-1})	Possible Assignment	Related Process Occurring
600-800	Ti-O-Ti vibrations	Different vibration modes of TiO_2
1300-1400	Stretching vibrations of O-H groups	Physically absorbed moisture

Table 5 Identification of Peaks from FTIR

4.3.5 N_2-physisorption (BET)

All the samples displayed Type III isotherm. They are usually characterized as having weak interaction between the adsorbent and the adsorbate. With reference to the effect of calcination temperature, we observed the surface area for each of the 0.1Fe-0.4Zn/TiO_2 calcined at different temperatures; 200˚C, 300˚C and 400˚C.

Photocatalyts	BET surface area (m^2g^{-1})	Total pore volume (cm^3g^{-1})	Average pore diameter (nm)
0.1Fe-0.4Zn/TiO_2			
200 ˚C	12.126	0.0042679	1.9981
300 ˚C	17.042	0.043676	20.884
400 ˚C	11.451	0.0020754	1.6187
Bare Anatase TiO_2	9.7793	0.010617	5.2641

As compared to bare TiO_2, the metal doped catalysts showed higher surface area. The best performing photocatalyst, 01Fe-0.4Zn/TiO_2 calcined at 300˚C showed the highest surface area, pore volume and pore diameter. The higher area available for contact of reactants id directly related to its high photocatalytic activity.

5.0 Conclusion

The objectives of this project have been met and conclusion is based on the two separate parts of this study respectively.

I. Synthesis Optimization

The best photocatalyst (COD removal 66.5%) was synthesized using Wet Impregnation method, using Anatase Titania with best metal composition of 0.1Fe-0.4Zn.

II Parametric Optimization

Photocatalyst calcined at 300˚C gave the highest activity; its activity decreases with increasing DIPA concentration & increases with time.

However, I believe this study could be a continuous one with rooms for improvements. Due to time limitations, the exact optimum condition for the effect of DIPA concentration and irradiation time could not be obtained. If experiments were repeated for more variables in the respective manipulated parameters until a certain constant pattern is obtained, it would be possible to conclude by stating the optimum conditions. Moreover, there are other parameters which can also be tested in this similar study such as the effect of photocatalyst loading, effect of pH and so on.

The scope of work of this project can be extended for further studies.

References

Ahmed, S., Rasul, M. G., Martens, W. N., Brown, R., & Hashib, M. A. (2010). Advances in Heterogeneous Photocatalytic Degradation of Phenols and Dyes in Wastewater: A Review. *Water, Air, & Soil Pollution, 215*(1-4), 3-29. doi: 10.1007/s11270-010-0456-3

Alfons, V., & Kim, S.-M. (2003). Advanced Oxidation Processes (AOPs) in Wastewater Treatment. *J. Ind. Eng. Chem., 10*(1), 33-40.

Arana, J., Diaz, O. G., Saracho, M. M., Rodriguez, J. M. D., Melian, J. A. H., & Pena, J. P. (2001). Photocatalytic degradation of formic acid using Fe/TiO2 catalysts: the role of Fe3+/Fe2+ ions in the degradation mechanism. *Applied Catalysis B: Environmental, 32*(1-2), 49-61. doi: 10.1016/s0926-3373(00)00289-7

Chen, C., Wang, Z., Ruan, S., Zou, B., Zhao, M., & Wu, F. (2008). Photocatalytic degradation of C.I. Acid Orange 52 in the presence of Zn-doped TiO2 prepared by a stearic acid gel method. *Dyes and Pigments, 77*(1), 204-209. doi: http://dx.doi.org/10.1016/j.dyepig.2007.05.003

Deshai Botheju, Yuan Li, Jon Hovland, Hans Aksel Haugen, Rune Bakke, & Biological treatment of amine wastes generated in post combustion CO2 capture.

Herrmann, J.-M. (2010). Photocatalysis fundamentals revisited to avoid several misconceptions. *Applied Catalysis B: Environmental, 99*(3-4), 461-468. doi: 10.1016/j.apcatb.2010.05.012

Kumar, S. G., & Devi, L. G. (2011). Review on Modified TiO2 Photocatalysis under UV/Visible Light: Selected Results and Related Mechanisms on Interfacial Charge Carrier Transfer Dynamics. *The Journal of Physical Chemistry A, 115*(46), 13211-13241. doi: 10.1021/jp204364a

Li, Y., Zhang, L., Wu, W., Dai, P., Yu, X., Wu, M., & Li, G. (2014). Hydrothermal growth of TiO2 nanowire membranes sensitized with CdS quantum dots for the enhancement of photocatalytic performance. *Nanoscale Res Lett, 9*(1), 270. doi: 10.1186/1556-276X-9-270

Liu, G., Wang, Z., Zheng, W., Yang, S., & Sun, C. (2014). Visible-Light-Driven Photocatalytic Degradation of Aniline over NaBiO 3. *Advances in Condensed Matter Physics, 2014*, 5. doi: 10.1155/2014/961609

Liu, W.-J., Zeng, F.-X., Jiang, H., Zhang, X.-S., & Li, W.-W. (2012). Composite Fe2O3 and ZrO2/Al2O3 photocatalyst: Preparation, characterization, and studies on the photocatalytic activity and chemical stability. *Chemical Engineering Journal, 180*(0), 9-18. doi: http://dx.doi.org/10.1016/j.cej.2011.10.085

Moioli, S., Pellegrini, L. A., & Gamba, S. (2012). Simulation of CO2 Capture by MEA Scrubbing with a Rate-Based Model. *Procedia Engineering, 42*(0), 1651-1661. doi: http://dx.doi.org/10.1016/j.proeng.2012.07.558

Obata, K., Kishishita, K., Okemoto, A., Taniya, K., Ichihashi, Y., & Nishiyama, S. (2014). Photocatalytic decomposition of NH3 over TiO2 catalysts doped with Fe. *Applied Catalysis B: Environmental, 160–161*(0), 200-203. doi: http://dx.doi.org/10.1016/j.apcatb.2014.05.033

Ohtani, B. (2010). Photocatalysis A to Z—What we know and what we do not know in a scientific sense. *Journal of Photochemistry and Photobiology C: Photochemistry Reviews, 11*(4), 157-178. doi: 10.1016/j.jphotochemrev.2011.02.001

Omar, A. A., Ramli, R. M., & Khamaruddin, P. N. F. M. (2010). Fenton Oxidation of Natural Gas Plant Wastewater. *Canadian Journal on Chemical Engineering & Technology, 1*(1).

Pei, C. C., & Leung, W. W.-F. (2013). Photocatalytic degradation of Rhodamine B by TiO2/ZnO nanofibers under visible-light irradiation. *Separation and Purification Technology, 114*(0), 108-116. doi: http://dx.doi.org/10.1016/j.seppur.2013.04.032

Pellegrini, L. A., Moioli, S., & Gamba, S. (2011). Energy saving in a CO2 capture plant by MEA scrubbing. *Chemical Engineering Research and Design, 89*(9), 1676-1683. doi: http://dx.doi.org/10.1016/j.cherd.2010.09.024

Poste, A. E., Grung, M., & Wright, R. F. (2014). Amines and amine-related compounds in surface waters: A review of sources, concentrations and aquatic toxicity. *Science of The Total Environment, 481*(0), 274-279. doi: http://dx.doi.org/10.1016/j.scitotenv.2014.02.066

Putri, F. K., Bustam, M. A., & Omar, A. A. (2011). Using Fenton's Reagants for the Degradation of Diisopropanolamine: EFfect of Temperature and pH. *International Conference on Environment and Industrial Innovation, 12*.

Qi, X.-H., Wang, Z.-H., Zhuang, Y.-Y., Yu, Y., & Li, J.-l. (2005). Study on the photocatalysis performance and degradation kinetics of X-3B over modified titanium dioxide. *Journal of Hazardous Materials, 118*(1–3), 219-225. doi: http://dx.doi.org/10.1016/j.jhazmat.2004.11.007

Ramli, R. M., Chong, F. K., & Omar, A. A. (2014). Visible-Light Photodegradation of Diisopropanolamine Using Bimetallic Cu-Fe/TiO2 Photocatalyst. *Advanced Materials Research, 845*, 421-425.

Riaz, N., Bustam, M. A., Chong, F. K., Man, Z. B., Khan, M. S., & Shariff, A. Photocatalytic degradation of DIPA using bimetallic Cu-Ni/TiO2 photocatalyst

under visible light irradiation

Riaz, N., Chong, F. K., Man, Z. B., Khan, M. S., & Dutta, B. K. (2013). Photodegradation of Orange II under Visible Light Using Cu–Ni/TiO2: Influence of Cu:Ni Mass Composition, Preparation, and Calcination Temperature. *Industrial & Engineering Chemistry Research, 52*(12), 4491-4503. doi: 10.1021/ie303255v

Safari, M., Nikazar, M., & Dadvar, M. (2013). Photocatalytic degradation of methyl tert-butyl ether (MTBE) by Fe-TiO2 nanoparticles. *Journal of Industrial and Engineering Chemistry, 19*(5), 1697-1702. doi: http://dx.doi.org/10.1016/j.jiec.2013.02.008

Sayari, A., Belmabkhout, Y., & Serna-Guerrero, R. (2011). Flue gas treatment via CO2 adsorption. *Chemical Engineering Journal, 171*(3), 760-774. doi: http://dx.doi.org/10.1016/j.cej.2011.02.007

Siuleiman, S., Kaneva, N., Bojinova, A., Papazova, K., Apostolov, A., & Dimitrov, D. Photodegradation of Orange II by ZnO and TiO2 powders and nanowire ZnO and ZnO/TiO2 thin films. *Colloids and Surfaces A: Physicochemical and Engineering Aspects*(0). doi: http://dx.doi.org/10.1016/j.colsurfa.2014.01.010

Thiruvenkatachari, R., Vigneswaran, S., & Moon, I. (2008). A review on UV/TiO2 photocatalytic oxidation process (Journal Review). *Korean Journal of Chemical Engineering, 25*(1), 64-72. doi: 10.1007/s11814-008-0011-8

Tryba, B., Morawski, A. W., Inagaki, M., & Toyoda, M. (2006). The kinetics of phenol decomposition under UV irradiation with and without H2O2 on TiO2, Fe–TiO2 and Fe–C–TiO2 photocatalysts. *Applied Catalysis B: Environmental, 63*(3-4), 215-221. doi: 10.1016/j.apcatb.2005.09.011

Wang, L., Wang, Z., Wang, D., Shi, X., Song, H., & Gao, X. (2014). The photocatalysis and mechanism of new SrTiO3/TiO2. *Solid State Sciences, 31*, 85-90. doi: 10.1016/j.solidstatesciences.2014.03.005

Yoong, L. S., Chong, F. K., & Dutta, B. K. (2009). Development of copper-doped TiO2 photocatalyst for hydrogen production under visible light. *Energy, 34*(10), 1652-1661. doi: http://dx.doi.org/10.1016/j.energy.2009.07.024

Yuan, Z.-h., Jia, J.-h., & Zhang, L.-d. (2002). Influence of co-doping of Zn(II)+Fe(III) on the photocatalytic activity of TiO2 for phenol degradation. *Materials Chemistry and Physics, 73*(2–3), 323-326. doi: http://dx.doi.org/10.1016/S0254-0584(01)00373-X

Zhao, C., Pelaez, M., Dionysiou, D. D., Pillai, S. C., Byrne, J. A., & O'Shea, K. E. (2014). UV and visible light activated TiO2 photocatalysis of 6-hydroxymethyl uracil, a model compound for the potent cyanotoxin cylindrospermopsin. *Catalysis Today, 224*, 70-76. doi: 10.1016/j.cattod.2013.09.042

Zhi, R., Bustam, M. A., Riaz, N., & Shariff, A. (2014). Efficiency of Visible Light Assisted Fenton Oxidation of Diisopropanolamine (DIPA) of Natural Gas Industry Wastewater. *Advanced Materials Research, 845*, 477-481.